

AD-A061 982

METEOROLOGY INTERNATIONAL INC MONTEREY CALIF

F/G 20/1

INTERFERENCE OF ARRIVALS IN CONTINUOUS WAVE TRANSMISSION EXPERI--ETC(U)

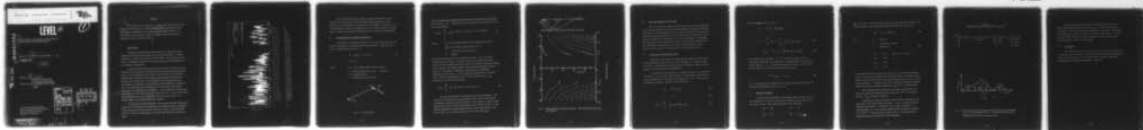
NOV 68 C S CLAY

N00228-68-C-2406

NL

UNCLASSIFIED

1 OF 1
AD
A061982



END
DATE
FILMED
2-79
DDC

METEOROLOGY INTERNATIONAL INCORPORATED

P. O. BOX 349 • MONTEREY, CALIFORNIA 93940



LEVEL III

①
ms

AD A061982

⑥
INTERFERENCE OF ARRIVALS IN CONTINUOUS
WAVE TRANSMISSION EXPERIMENTS.

⑨
Project M-153, Technical Note Four no. 4,

②
November 1968

⑫ 11p.

DDC FILE COPY

⑩
Prepared by: C. S. Clay
Professor of Geophysics
University of Wisconsin

Under Contract No. N00228-68-C-2406

⑮

ACCESSION for	
DTB	White Section <input checked="" type="checkbox"/>
DDO	Buff Section <input type="checkbox"/>
UNANNOUNCED	<input type="checkbox"/>
JUSTIFICATION	
Per: Basic Rot.	
BY: AD-731235	
DISTRIBUTION/AVAILABILITY CODES	
Dist.	AVAIL. and/or SPECIAL
A	

DDC
RECEIVED
DEC 11 1978

For the Commanding Officer
Fleet Numerical Weather Central
Naval Postgraduate School
Monterey, California

DISTRIBUTION STATEMENT A
Approved for public release;
Distribution Unlimited

78 12 11 065
227 450
LB

Abstract

The emissions of sound energy in each of the ray paths leave the source at different angles. The frequencies of the signal traveling in these paths are different by the amount of their Doppler shift. The fluctuations of the received signal are caused by the interference of signals traveling by different paths.

I Introduction

If several different transmission paths exist, then the signals interfere and produce maxima and minima in the sound field. A simple interference is the surface dipole or Lloyds mirror. At large range in the ocean, a tremendous number of paths are possible and the interferences are extremely complicated.

Tolstoy and Clay (1966) discussed this problem in detail and have displayed many comparisons of theoretical and experimental transmission curves. At low frequencies and modes, they were able to theoretically determine the interference wavelengths and the ranges of maxima and minima in the sound field. At high frequencies and large range, the coincidence of computed and measured maxima and minima is a matter of luck. The theoretical and experimental curves had the same general appearance and interference wavelengths. Their comparison of experiment with theory for a 100 mode example is shown on Fig. 1. In the 60 to 70 km range the theoretical and experimental curves are very similar. At shorter ranges, even higher modes are important.

In Chapter 8 of *Ocean Acoustics*, they suggest that the interference effects can be studied by the application of spectrum analysis techniques to the mean square signal level as a function of range. This procedure should be easier than attempting to calculate the signal as a function of range.

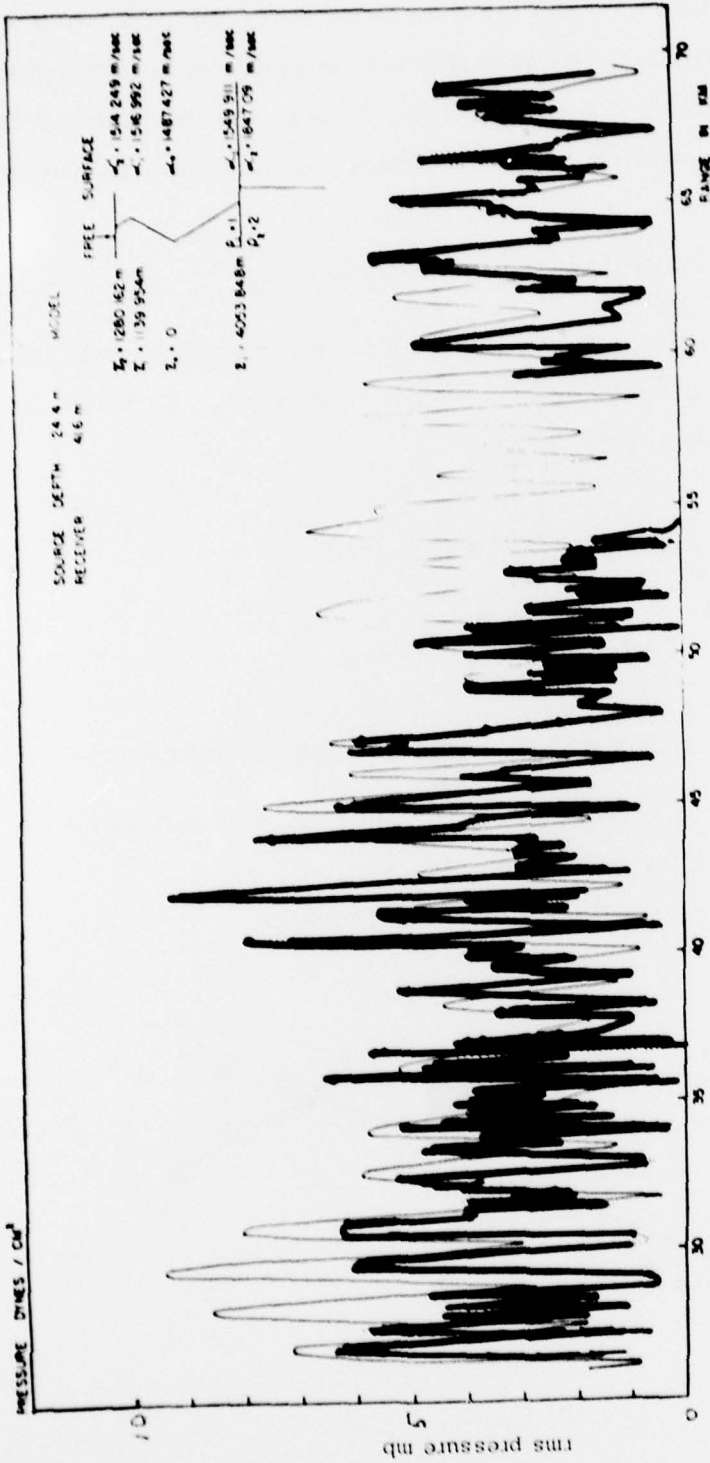


Fig. 3. Experimental and calculated (solid line) pressure amplitude versus range for a simple harmonic source at 10 cps at a depth of 24 m in a deep section of the ocean. After Guthrie et al. [1960]. This shows the complicated nature of the field variations that are found at even such low frequencies: at 10 cps we already have close to 100 guided modes in the model assumed for the calculations. (See Guthrie et al. [1960].)

Fig. 1 The power of the source was estimated to be about 50 watts. From Tolstoy and Clay, Ocean Acoustic: an evaluation, Rev. of Geophysics, 4, 33-40 (1966) and the monograph Ocean Acoustics, McGraw-Hill Book Co., New York (1966).

68 12 17 06 5

If the existing numerical methods for making long-range sound transmission computations used the normal mode formulation, then we could write the spectrum of the interferences immediately. However, most of the numerical methods are based on ray traces, thus we need to develop ways to use this information for the estimation of interference phenomena.

II Doppler effect and signal transmission

The change of frequency caused by source motion is well known and easy to demonstrate in underwater sound transmission. With the aid of Fig. 2, the shifted frequency ω' is

$$\omega' = \omega_0 (1 - v \cos \theta / c) \quad (1)$$

$$v/c \ll 1$$

where

$\omega_0 = 2\pi f_0$ is the source angular frequency

v is the velocity of the source, + outgoing

θ is defined on Fig. 2

c is velocity of sound in water

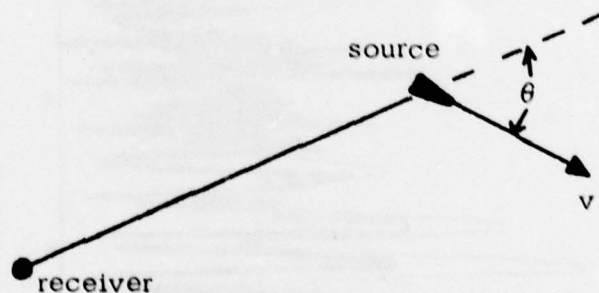


Fig. 2 Source motion

Let us designate the amplitude of the signal that travels along a particular path as being $s_m(r)$. The total signal at the receiver is the following sum of all contributions:

$$s(r, t) = \sum_{1}^M s_m(r) e^{i \varphi_m(r)} e^{i [\omega_0 (1 - v \cos \theta_m / c)] t} \quad (2)$$

where θ_m is the emission angle of the mth ray at the source
 $\varphi_m(r)$ is the phase of the signal at $t = 0$
 v is the velocity of the source
 M arrivals

Except for convergence zones and shadow regions, $s_m(r)$ is slowly varying function of range. The phase $\varphi_m(r)$ depends upon the exact number of wave lengths between the source and receiver, the phase change at all reflection and turning points, and diffractions caused by inhomogeneities. The phase is sensitive to internal waves and the time dependence of the ocean. For most practical purposes $\varphi(r)$ is random. Over a limited range increment $s_m(r)$ can be replaced by \bar{s}_m , φ_m ignored and Eq. (2) is the following:

$$s(t) = \sum_{1}^M \bar{s}_m \exp i [\omega_0 (1 - v \cos \theta_m / c)] t \quad (3)$$

The emission angles are obtained by ray tracing technique. The display of arrival angle or emission angle versus range is particularly convenient for making numerical studies. Such a plot for a source at the surface and receiver on the sound channel axis is shown on Fig. 3. The bottom reflections at angles greater than 30° have been ignored. At a given range, θ_m for all the arrivals can be read on the graph.

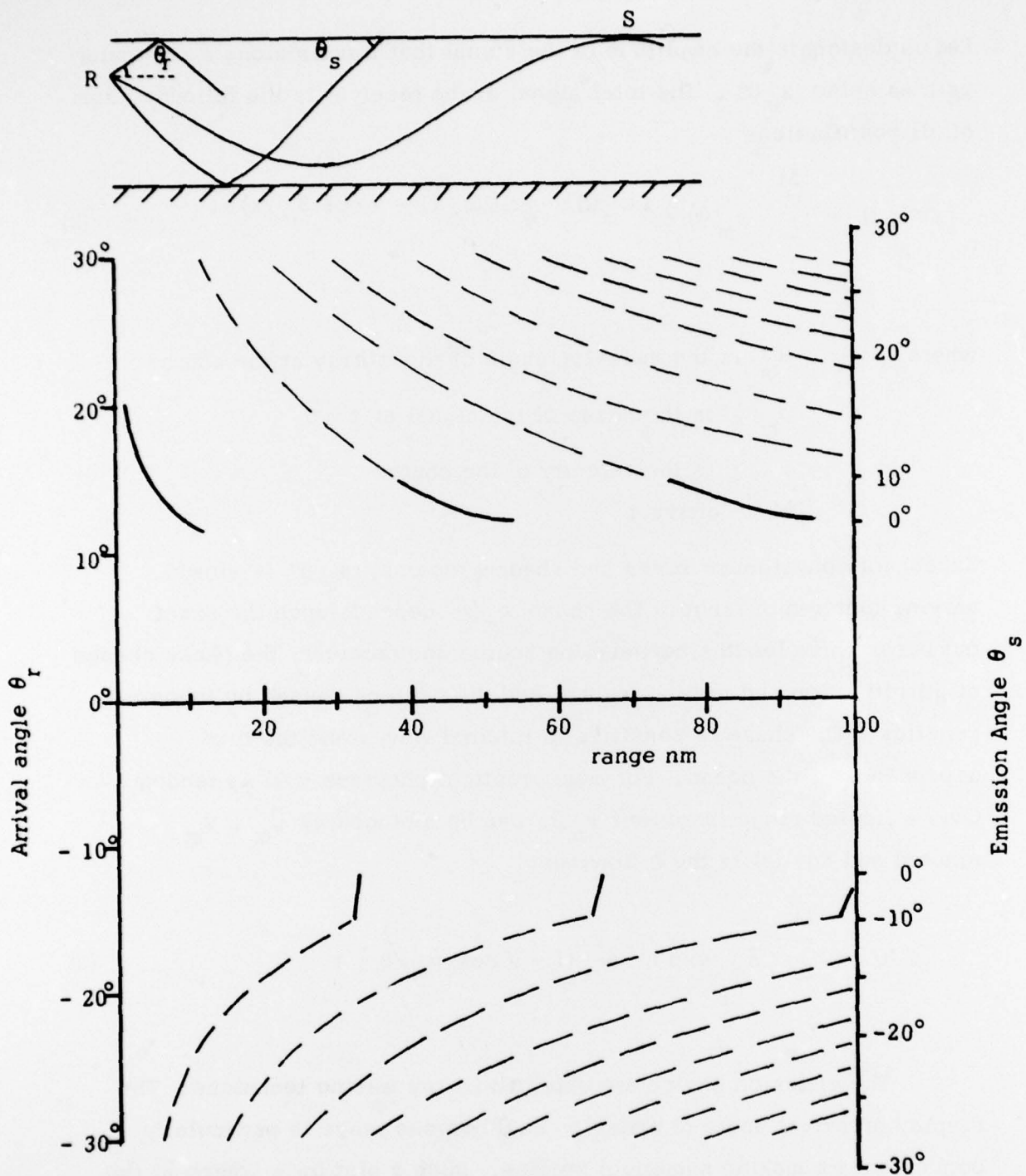


Fig. 3 Arrival angle as function of range. The bottom reflected parts are dashed.

III Spectrum analysis of the signal

The use of spectrum analysis of the signal to determine components of the Doppler shifted signals has some limitations and requires extremely good control. The frequency shifts are small and extremely long times are needed to measure the frequency. Since the source is moving, this means that the condition for small change of \bar{s}_m can be violated. Even though the separations of the components are very small, the mean shift of all of the components is appreciable. A number of measurements of source velocity have been made by measuring the average Doppler shift.

IV Fluctuations of the signal level

Numerous experiments have shown that the signal received from a moving continuous wave source has many fluctuations. In the ray path description, each path has a slightly different frequency and the received signal is the sum of all of the contributions.

To examine the signal level as a function of range, it is convenient to replace vt by r in the range increment. [The distance to the chosen range increment can be absorbed in the $\phi_m(r)$ in Eq. (2)]. With this and the following change of variable, Eq. (3) becomes:

$$k_m = \frac{\omega}{c} \cos \theta_m \quad (4)$$

$$r = vt \quad (5)$$

$$s(t) = \sum_1^M \bar{s}_m \exp i(\omega t - k_m r) \quad (6)$$

The mean square value of $s(t)$ is

$$s^2 = \frac{1}{T} \int_0^T s(t) s^*(t) dt$$

$$s^2 = \sum_1^M \bar{s}_m^2 + 2 \sum_{m > n} \bar{s}_m \bar{s}_n \cos \Delta k_{mn} r \quad (7)$$

$$\Delta k_{mn} \equiv k_m - k_n = \frac{\omega}{c} (\cos \theta_m - \cos \theta_n) \quad (8)$$

Over a short range increment s^2 is the sum of a mean level and a fluctuating component. The techniques of stationary time series analysis can be applied to s^2 to estimate the spatial spectrum. From Eq. (7), one can define a spatial spectrum function as follows:

$$S^2(\Delta k_{mn}) \equiv \bar{s}_m \bar{s}_n \quad (9)$$

Thus, experimental measurements of the spatial spectrum can be used to estimate the magnitude $\bar{s}_m \bar{s}_n$ in Eq. (7).

V Numerical example

To illustrate the magnitude of the numbers that might be expected in an experiment, we will use the range--emission angle graph, Fig. 3. At a range of 20 nm, the emission angles are the following:

$$\theta_1 = 20^\circ$$

$$\theta_2 = 15^\circ$$

$$\theta_3 = 28^\circ$$

$$\theta_4 = 23^\circ$$

(θ_1 and θ_3 are $+\theta$ arrival angles and θ_2 and θ_4 are the $-\theta$ angles). The frequency shifts Δf_m associated with θ_m are with the aid of Eq. (3)

$$\Delta f_m = f_o v \cos \theta_m / c \quad (10)$$

for

$$\begin{aligned} f_o &= 100 \text{ cps} \\ v &= 10 \text{ knots or } 5 \text{ m/sec} \\ c &= 1500 \text{ m/sec} \end{aligned} \quad (11)$$

$$\begin{aligned} \Delta f_1 &= 0.31 & \text{mean } \Delta f \approx 0.31 \text{ cps} \\ \Delta f_2 &= 0.32 \\ \Delta f_3 &= 0.29 \\ \Delta f_4 &= 0.31 \end{aligned}$$

It is evident that the mean frequency shift of 0.31 cps can be measured easily. If the source frequency were not known but if a hydrophone were located at right angles to the track, then approximate values of f_o can be used to estimate v . Analysis of the fine structure of the Doppler shifted signal would require spectrum analysis in about 10^{-3} cps band widths.

The interference wave numbers for the mean square level as a function of range are estimated with the aid of Eq. (8). For the same arrivals, Δk_{mn} are given on Table 1.

Actually one would not observe sharp spectral components in an experiment. The limited range increment Δr sets a minimum spectrum width of about $2\pi/(\Delta r)$. In addition, θ_m changes with range. On assuming that Δr is 1 nm, the half width of each component is roughly $0.3 \times 10^2 \text{ m}^{-1}$. The spectrum as shown on Fig. 4 is based upon the assumption that all arrivals have equal amplitude.

Table 1
Interference spatial frequencies Δk_{mn} in m^{-1}

n \ m	1	2	3	4
1	---	1.2×10^{-2}	2.3×10^{-2}	0.6×10^{-2}
2		---	3.5×10^{-2}	1.9×10^{-2}
3			---	1.7×10^{-2}

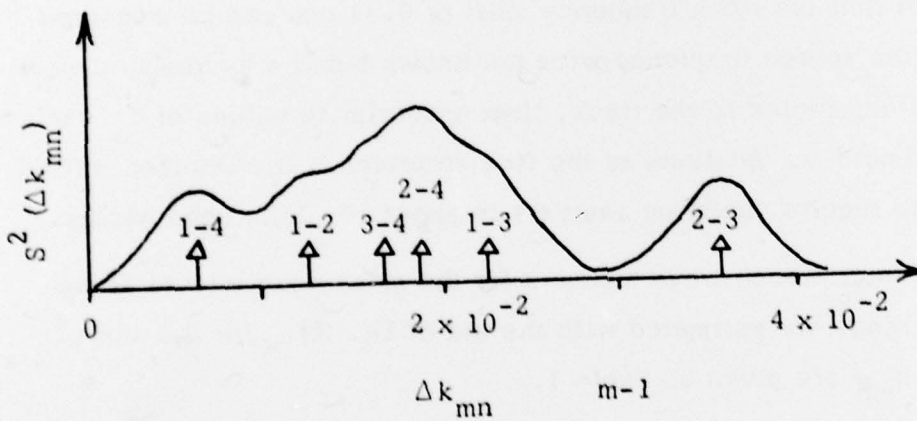


Fig. 4 Spectrum of the fluctuations: The location of the components Δk_{mn} are indicated by arrows. The components have been broadened and the total spectrum shown.

The two main interference peaks should be quite obvious. The short wavelength interference of $2\pi / \Delta k_{23} \approx 180$ m would be rather sinusoidal. The longer wavelength interference would have a more noise-like appearance and have a mean wave length of about 350m. Of course, for such a short range, the signal amplitudes are not equal and more dependent upon r than we have assumed.

VI A reflection

The ideas presented in this note are the result of many long range continuous wave experiments. When Ivan Tolstoy and I were preparing the text of Ocean Acoustics we were amazed at the paucity of published comparisons of theory and experiment. I still am.